Integrated Photonic Devices

http://ioe.eei.eng.osaka-u.ac.jp/

Advanced Integrated Photonic Devices

- IPD for Optical Network
- IPD for Ultrafast Signal Processing
- Quantum Structure Semiconductor Lasers
- Integrated Photonic Sensors
- Integrated Quantum Photonic Devices

Electron Beam Writing System for Photonics

Design Theory Simulation Fabrication Technology
Device Implementation・Experimental Demonstration

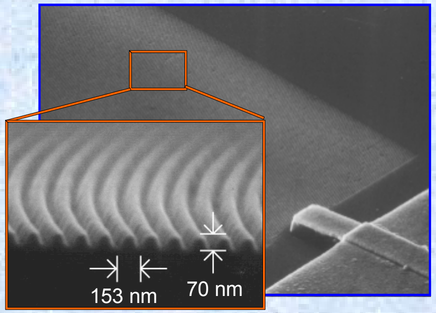

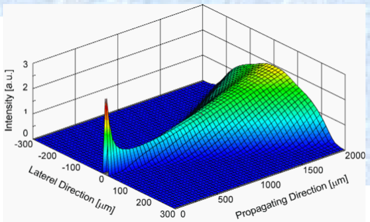

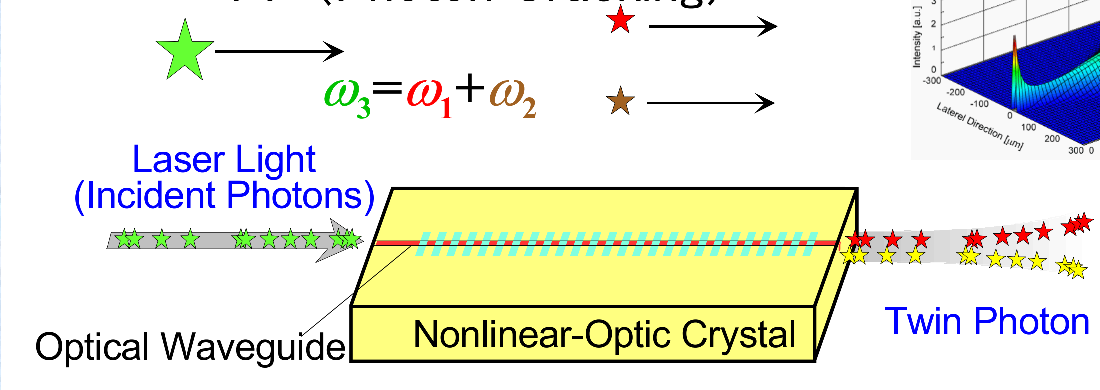

An Example of Quantum Photonic Devices

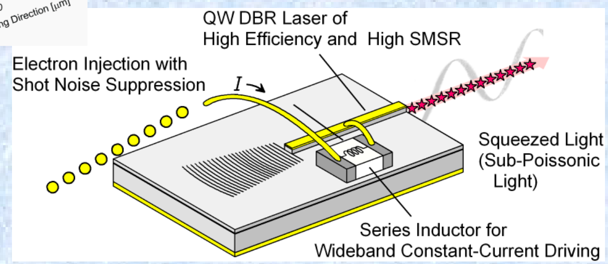

Integrated QW Semiconductor Laser

Waveguide Nonlinear-Optic Devices

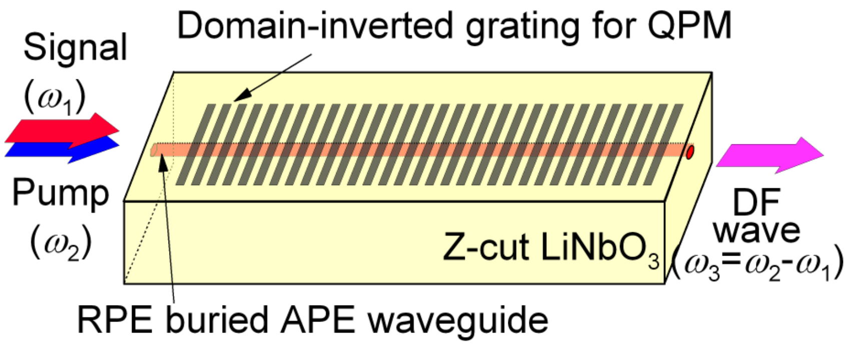

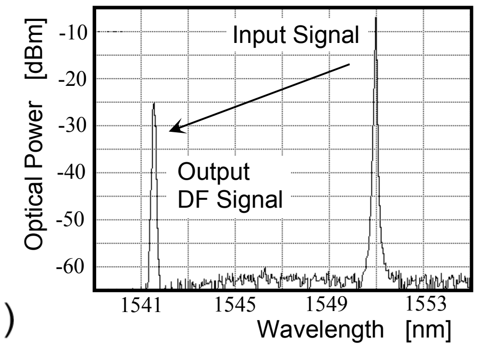

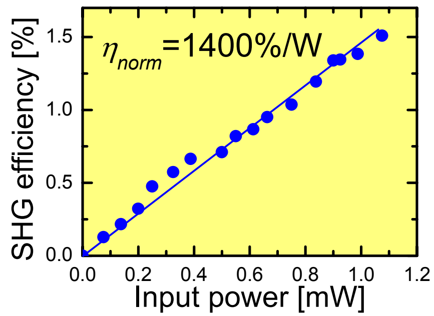

Top Data Efficiency

Wavelength Converters for Photonic Network

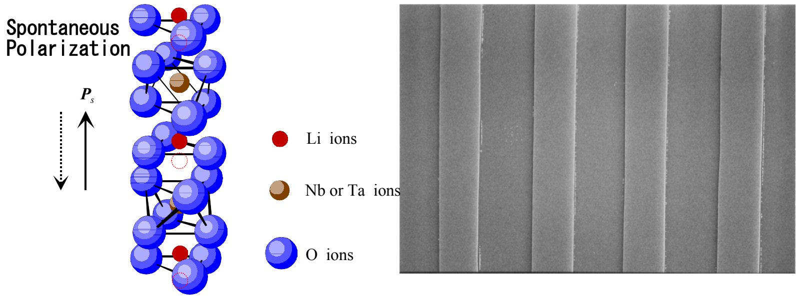

Domain Inverted Grating for QPM

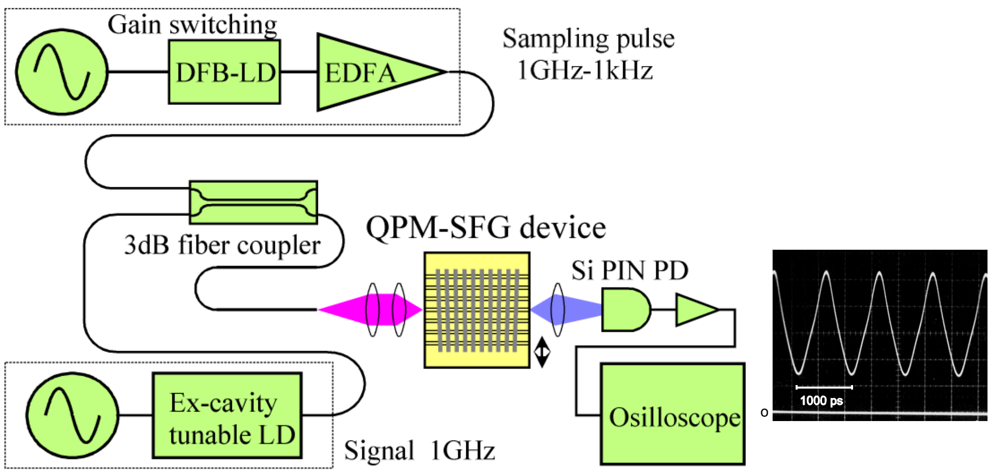

43%/W
Highest Efficiency

Optical Sampling Device

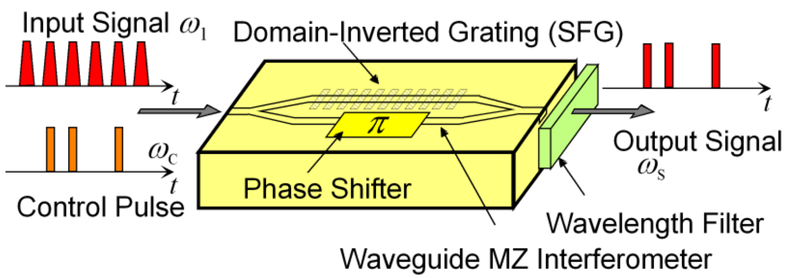

Ultrafast Optical Gate Switch

Ultrafast Optical-Signal Processing Devices

SFG Optical Sampling Device

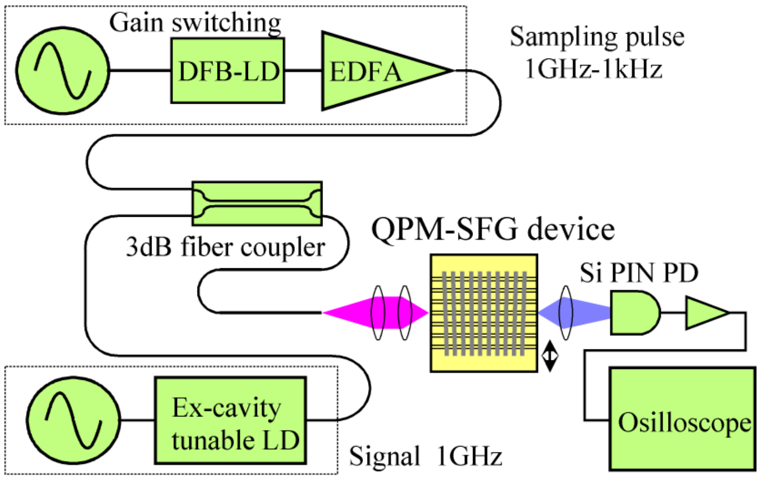

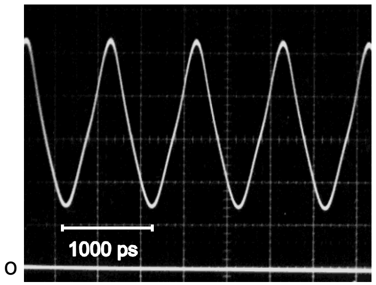

Waveform Observed
By Optical Sampling

Efficiency
43%/W

3-order of mag. higher
than with bulk crystal

T.Suhara et al. IEEE PTL **11**, 1027, 1999

SHG/DFG Optical Switching Device

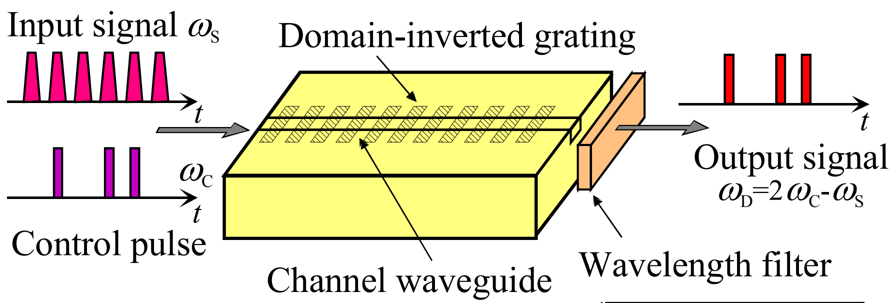

Spectrum of
Output Waves

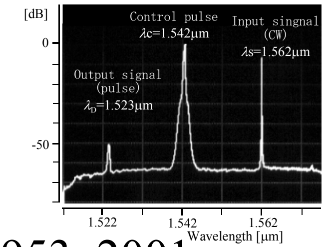

H.Ishizuki et al. OQE **33**, 953, 2001

SFG Interferometer Gate Switch

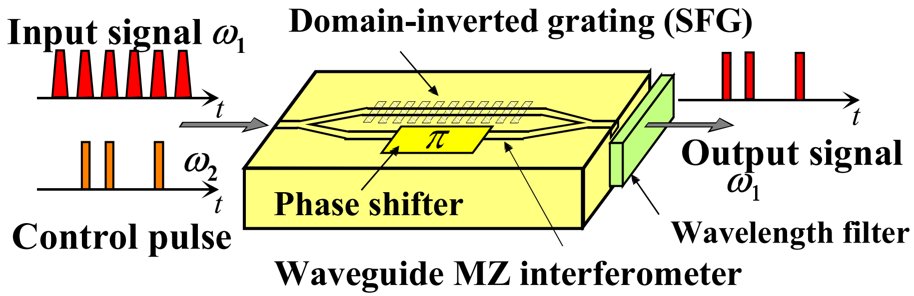

T.Suhara et al. IEEE PTL **13**, 1203, 2001

Formation of Domain-Inverted Grating for QPM

Voltage Pulse Application using Liquid Electrodes

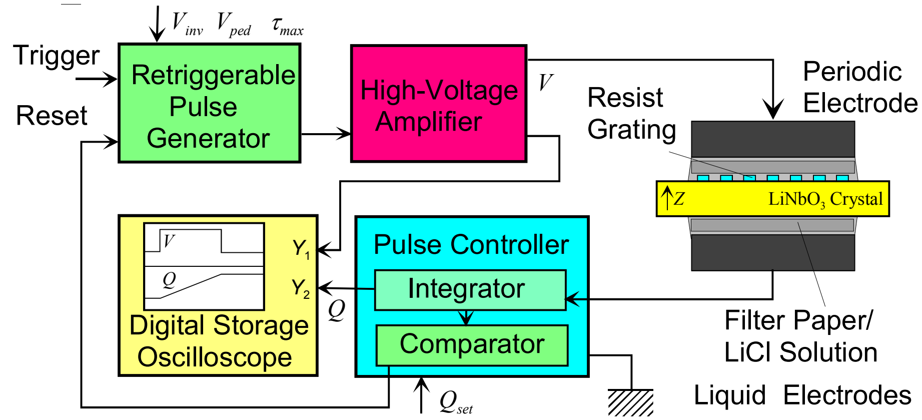

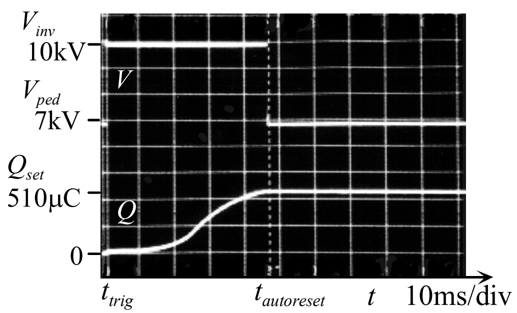

Voltage /Charge Traces

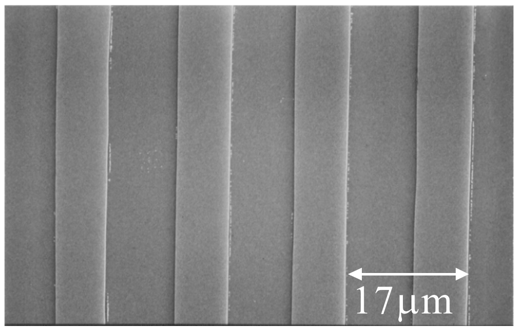

SEM Microphotograph
of Domain-Inverted Grating

Voltage Pulse Application using Metal Electrodes

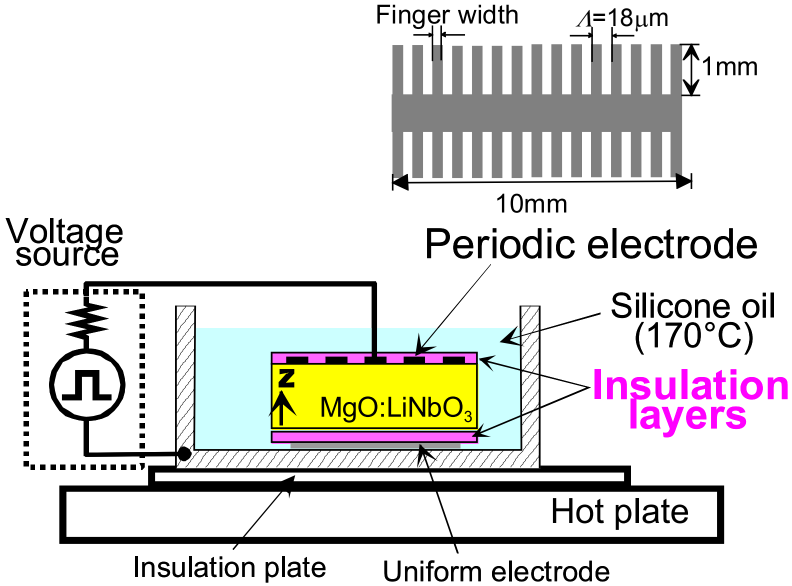

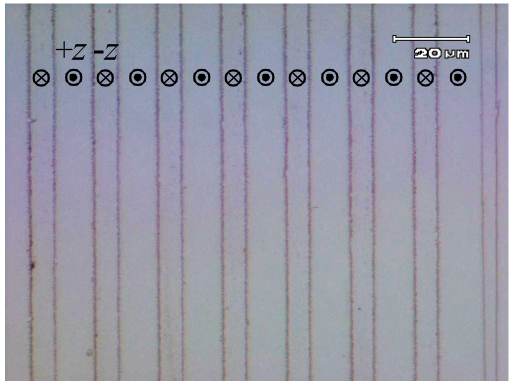

N.Horikawa, T. Tsubouchi, M.Fujimura
and T.Suhara, Jpn. J. Appl. Phys., 46, 5178, 2007.

QPM Grating Formation in $MgO:LiNbO_3$ Crystal

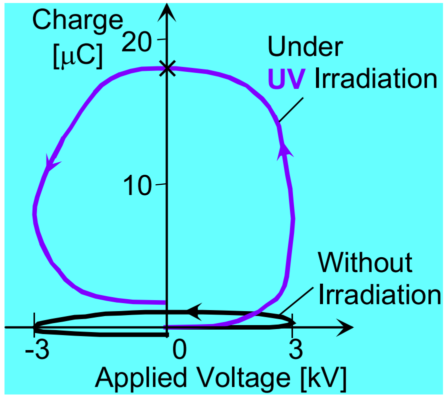

Ferroelectric Hysteresis Loop

$MgO:LiNbO_3$

PR damage resistant

UV Irradiation

Reduces

Eff. Coercive Field

Room Temperature Resistless Process

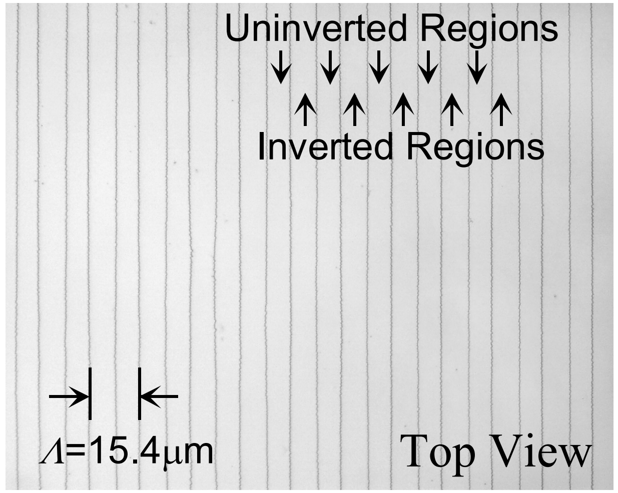

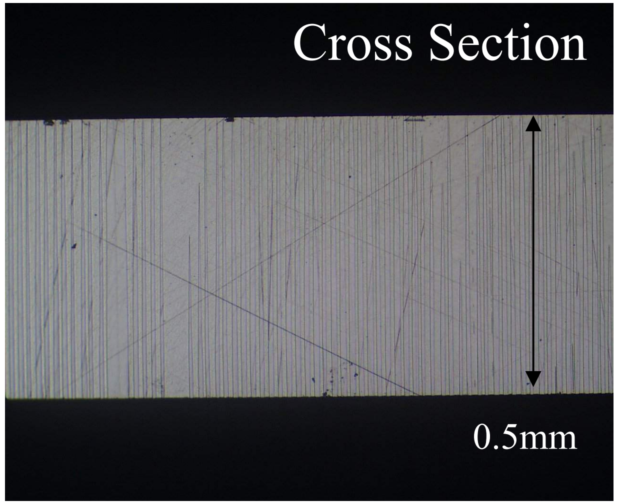

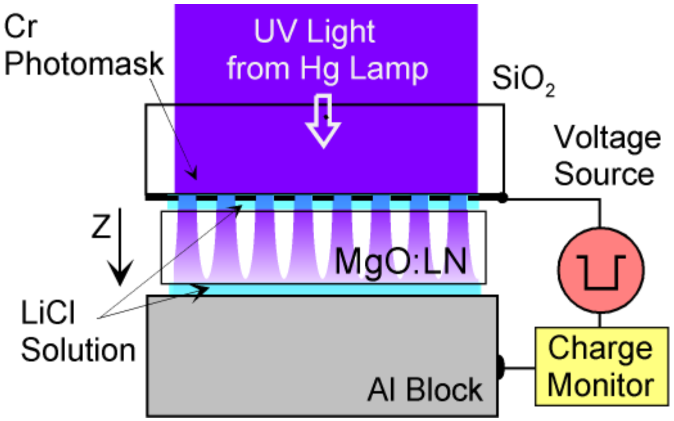

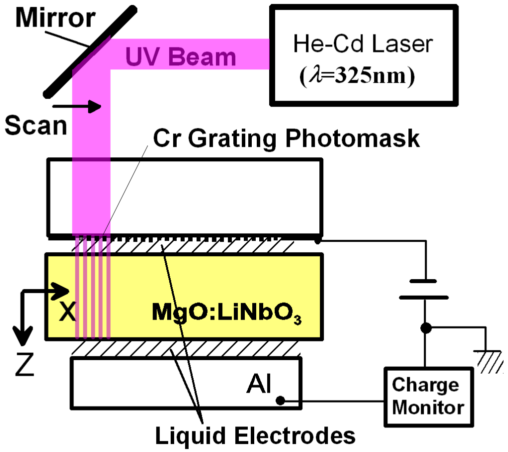

Formation of QPM Grating

M.Fujimura, T.Sohmura and T.Suhara EL. 39, 719, 2003

Fabrication of WG of strong confinement

Buried APE WG fabrication by direct bonding

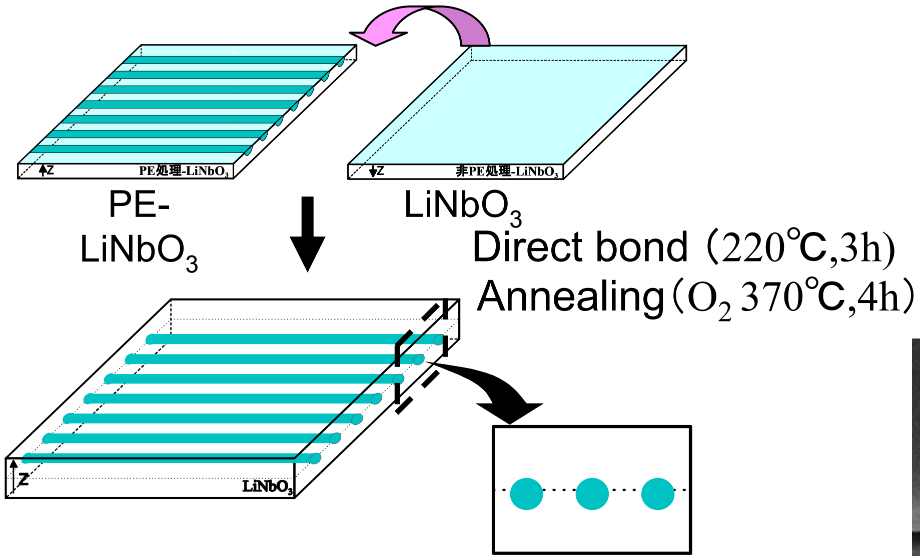

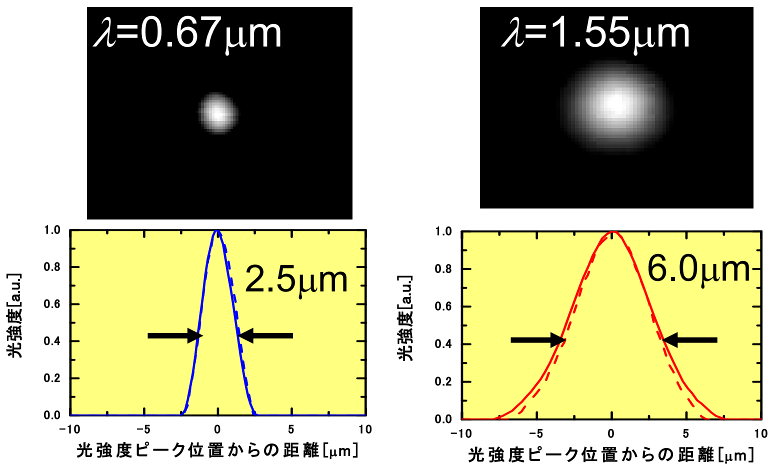

M.Fujimura et al. EL **44**, 856 2008

Ridge WG fabrication by PE accelerated chemical etching

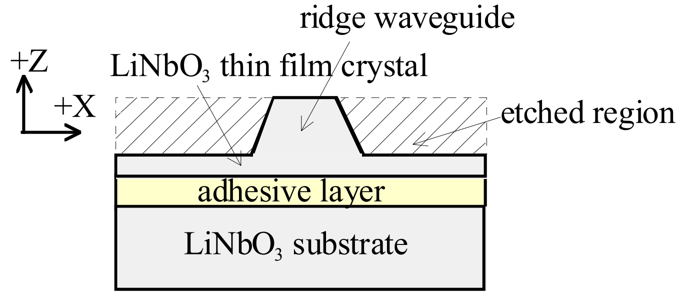

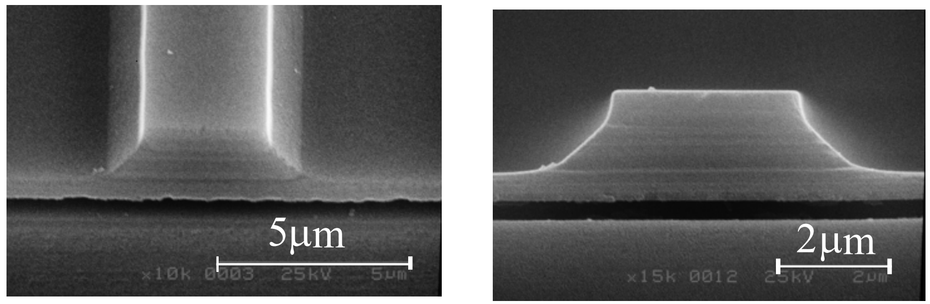

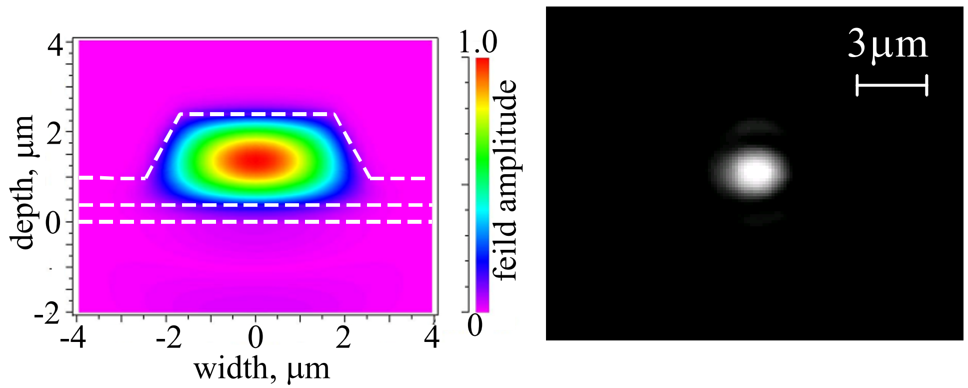

T.Takaoka et al. EL **45**, 940 2009

Quantum Photonic Devices

Efficient Integrated Photonic Devices for Quantum Optic Function

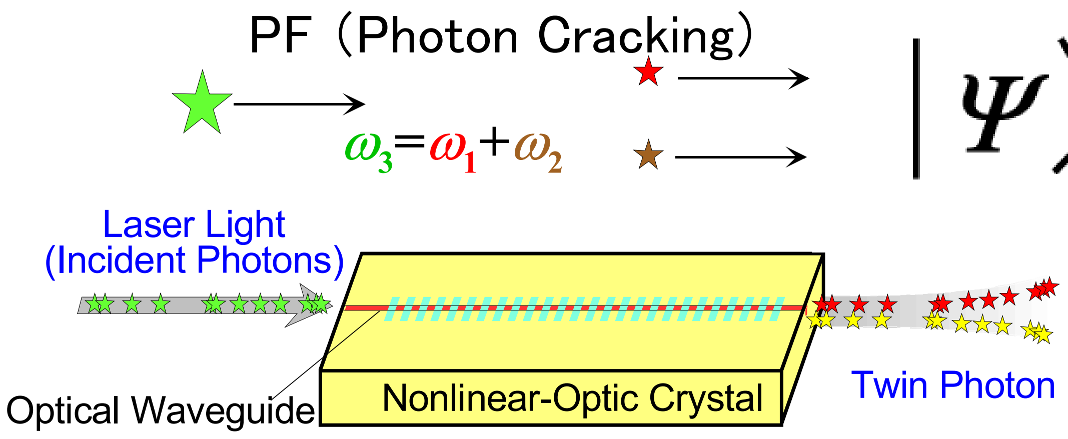

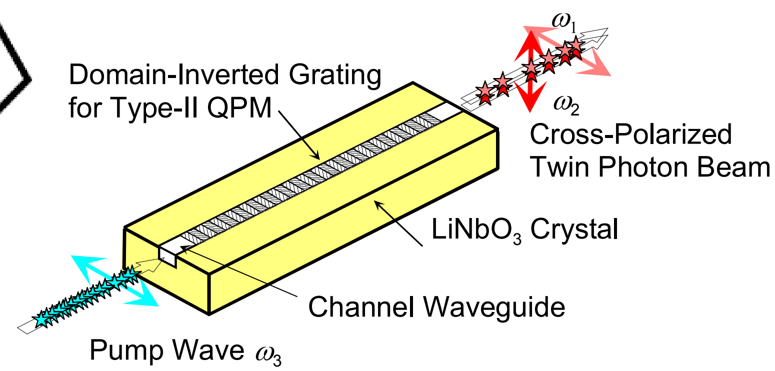

Correlated Twin-Photon Generation

- **Entangled Photon Generation**
- **Single Photon Generation**

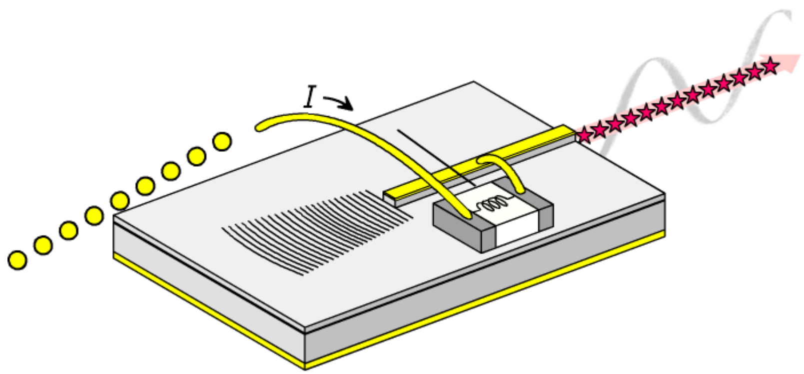

Squeezed Light Semiconductor Laser

Applications
Quantum Information
Quantum Cryptography
Quantum Computing
Quantum Photonic Sensing

QPM WG SFG upconversion device for single photon detection

QIT Photon transmission through fiber network

Telecom (1.3, 1.5μm) band **Single photon detector**

InGaAs-APD involve drawbaks

SFG upconversion to visible and detection by Si-APD

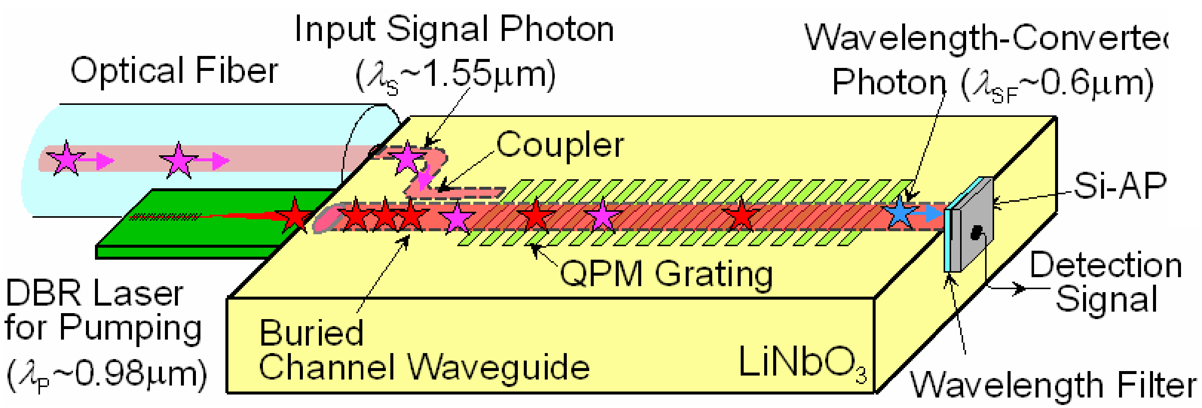

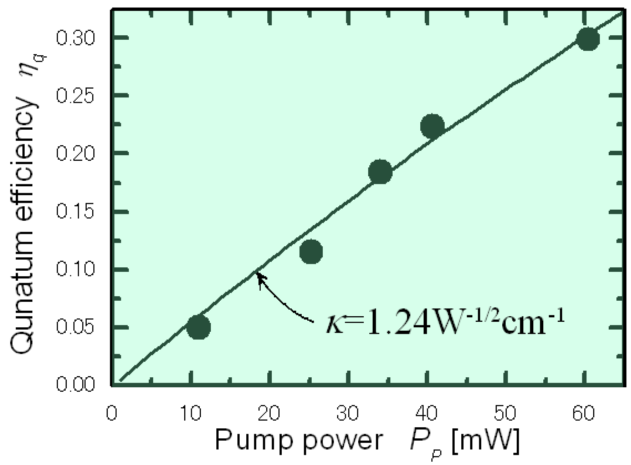

η~30% @P_p=60mW

M.Fujimura, et al. JJAP **46**, 9A, 5868, 2007

WG QPM Entangled Twin Photon Generation Devoces

QPM Waveguide NLO Devices for Quantum Information Processing
Q-Cryptography, Q-Teleportation, Q-Interface, …

Quantum Entangled Twin Photons

high efficiency, wavelength flexibility
Integration compatibility

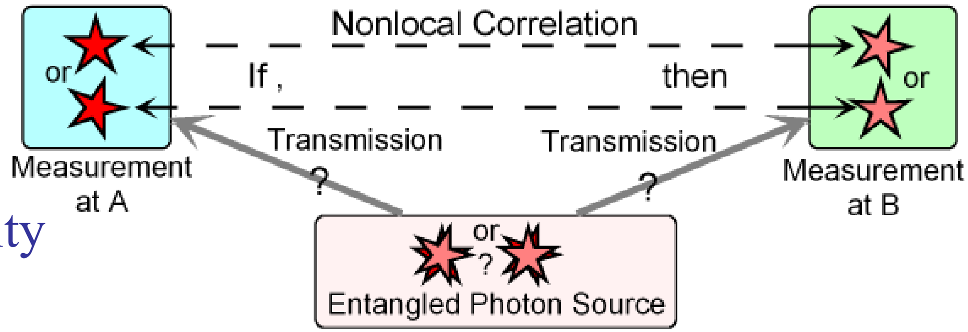

Key Devise for QIT

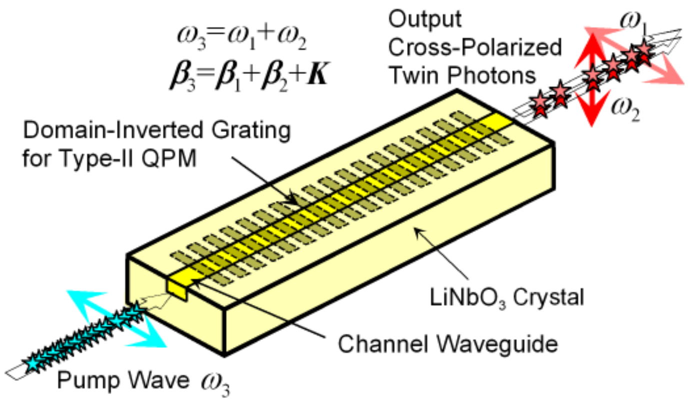

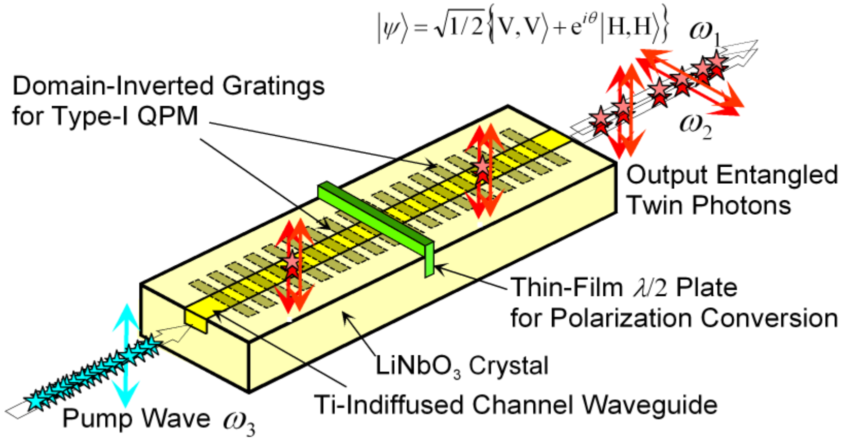

T.Suhara et al. IEEE PTL **19**, p.1093,2007.   J.Kawashima et al., IEEE PTL., **21,** p.566, 2009.

Quantum theory analysis of TPG

Quantum coupled mode eq (H.P.)

$$\frac{d}{dz}a_1(z) = i\kappa A_3 a_2^{\dagger}(z)\exp(i2\Delta z)$$

$$\frac{d}{dz}a_2(z) = i\kappa A_3 a_1^{\dagger}(z)\exp(i2\Delta z)$$

$$\langle N_1(L)\rangle = \langle N_2(L)\rangle = \sinh^2 \Gamma L\{\sin \Delta L/\Delta L\}^2$$

$$P_{out1} = \hbar\omega_1 \int \langle N_1(L)\rangle (d\omega_1/2\pi) \text{ in QPM bandwidth}$$

Photon CCR

$$P_c(\tau) \propto \mathrm{rect}\left(2\frac{\delta\omega}{2\pi}\tau\right)$$

Correlation time

$$\tau_c = (\delta\omega/2\pi)^{-1} = |n_1 - n_2|L/c$$

Unitary transformation of state (S.P.)

$$|\phi(L)\rangle = T(L)|0,0\rangle = \exp(-iHL)\,|0,0\rangle$$

$$= \sum_{n=0}^{\infty}\frac{1}{n!}(-iHL)^n|0,0\rangle$$

$$H = i\{a_1^{\dagger}(\Gamma e^{i\phi}a_2^{\dagger} - i\Delta a_1) - (\Gamma e^{-i\phi}a_1 + i\Delta a_2^{\dagger})\,a_2\}$$

$$|\phi(L)\rangle = \sum_{n=0}^{\infty}\sqrt{1-|r|^2}\,r^n|n,n\rangle$$

$$r = \frac{e^{i\phi}(\Gamma/\gamma)\sinh\gamma L}{\cosh\gamma L + i(\Delta/\gamma)\sinh\gamma L}$$

$$\langle[\Delta\{N_1(L) - N_2(L)\}]^2\rangle = 0$$

complete correlation

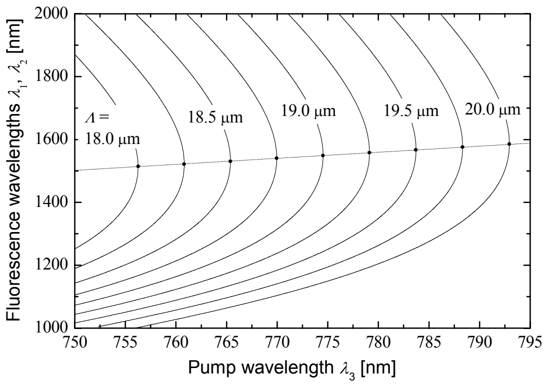

TM→TM+TM Type-I QPM

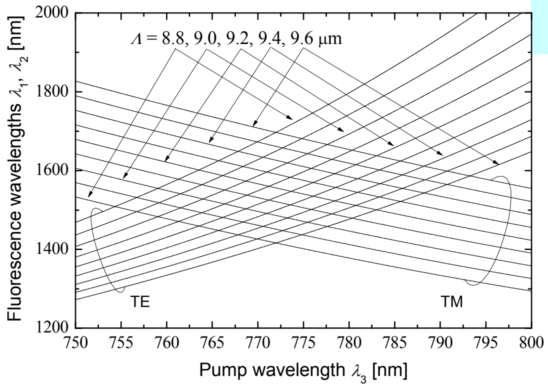

TE→TM+TE Type-II QPM

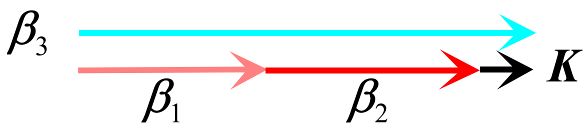

T.Suhara et al. IEEE JQE, **41**, 1203, 2005; **42**, 777, 2006

Type-II QPM Cross-Polarized TPG Device

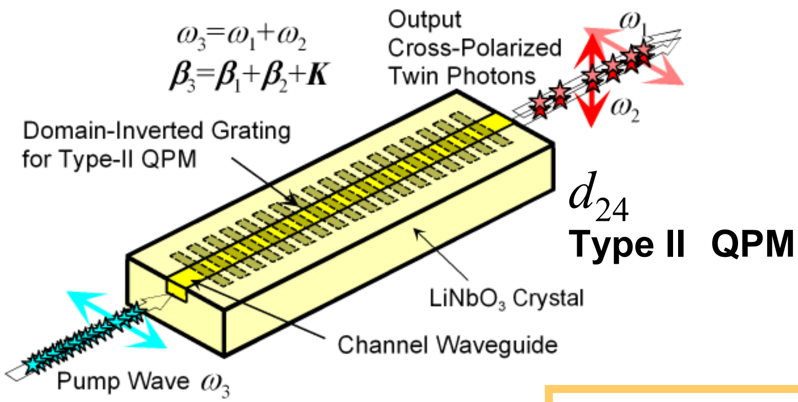

$\eta \sim 3\times10^{-10}$

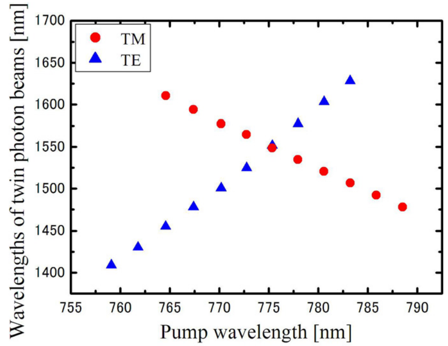

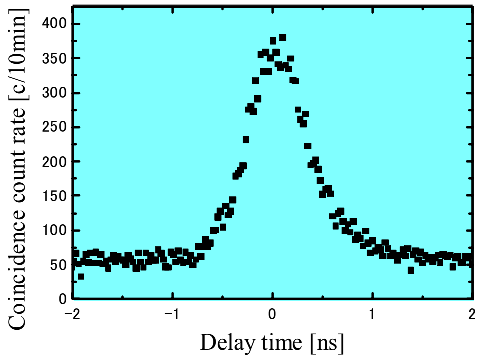

Photon Correlation

T.Nosaka et al. IEEE PTL, **18**, 1, p.124, 2006

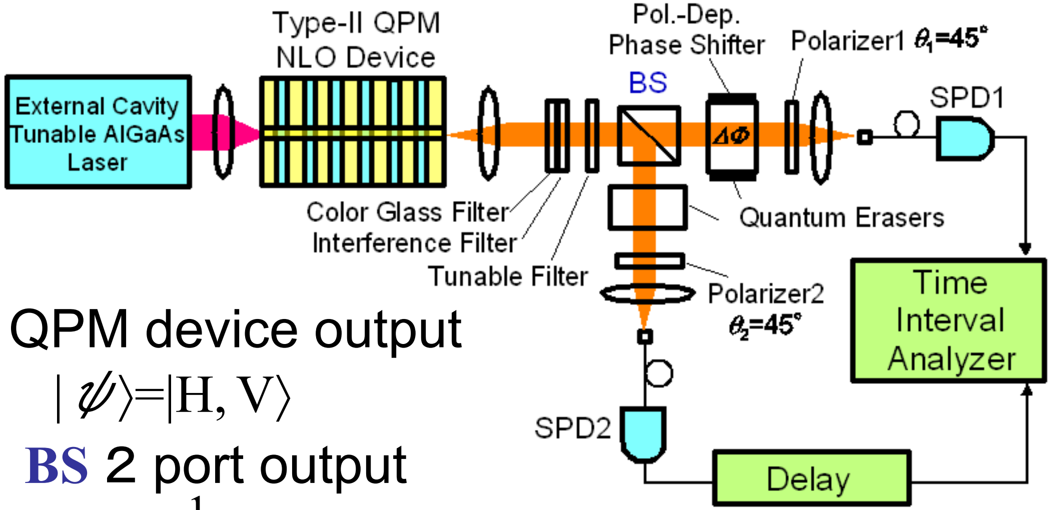

QPM device output

$|\psi\rangle=|H, V\rangle$

BS 2 port output

$$|\psi\rangle=\frac{1}{\sqrt{2}}\{|H;V\rangle-\exp(i\Delta\Phi)|V;H\rangle\}$$

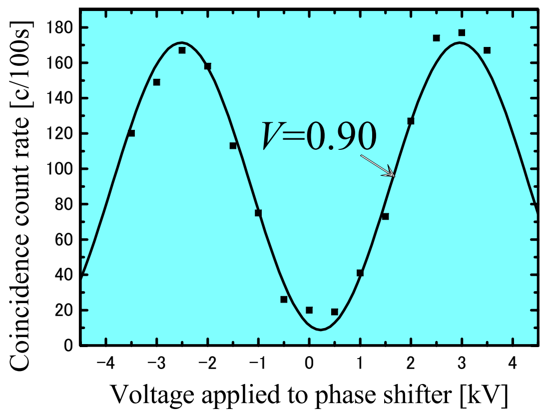

Quantum Interference

Polarization Entangled TPG

T.Suhara et al. IEEE PTL, **19**, 1093, 2007

Type I QPM Polarization-Entangled TPG Device

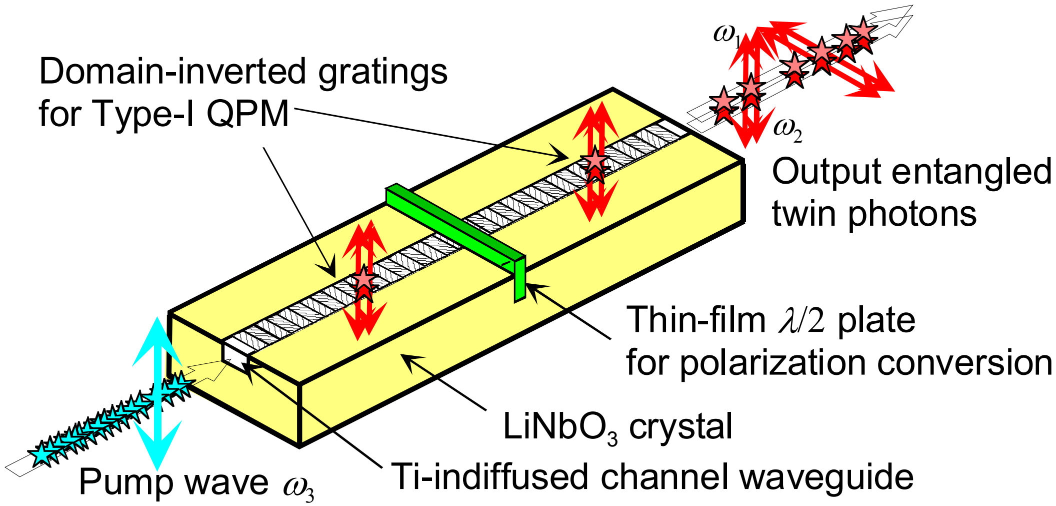

QPM device output

$$|\psi\rangle = \sqrt{1/2}\,\{|H,H\rangle + \exp(i\Phi_0)|V,V\rangle\}$$

BS output 1,2 state

$$|\psi\rangle = \sqrt{1/2}\{|H;H\rangle - \exp(i\Phi)\,|V;V\rangle\}$$

Quantum entangled state

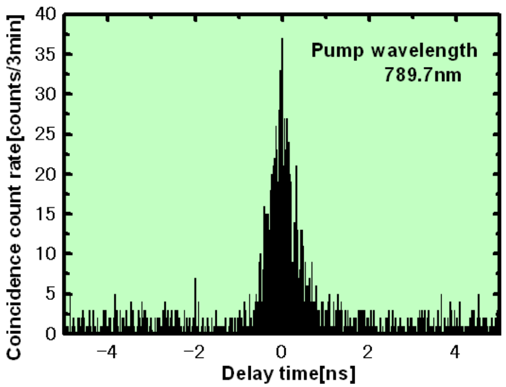

Photon correlation

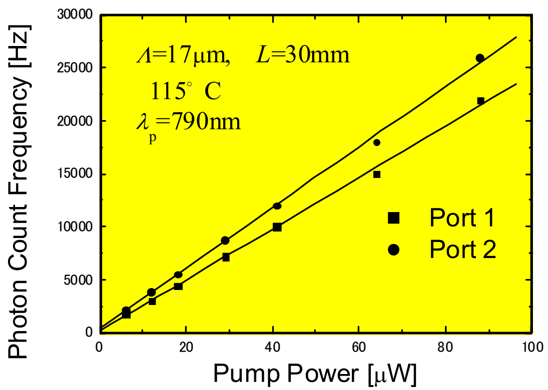

η=**2.4×10^{-7}** (theory 1.7×10^{-6})
High Efficiency higher than TypeII QPM by 3 orders of magnitude

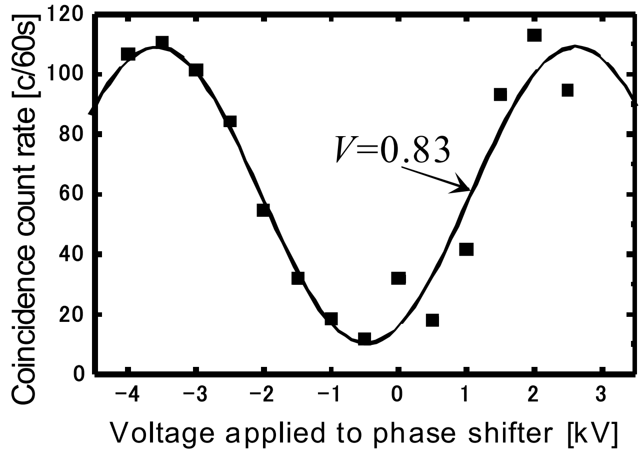

Quantum Interference demonstrating entangled TPG

J.Kawashima et al. IEEE PTL **21**, 566, 2009

QPM WG Devices for Generation of Postselection-Free Polarization-Entangled Twin Photons

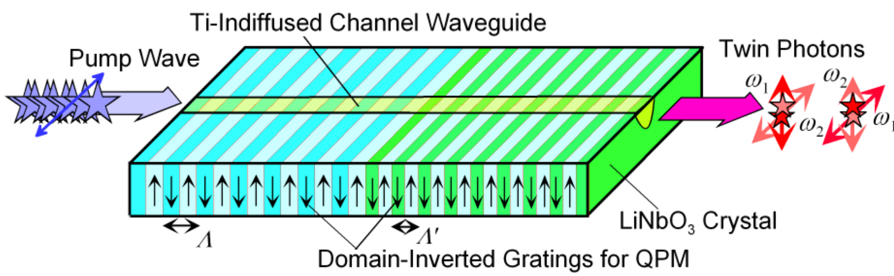

(a) Biperiod type

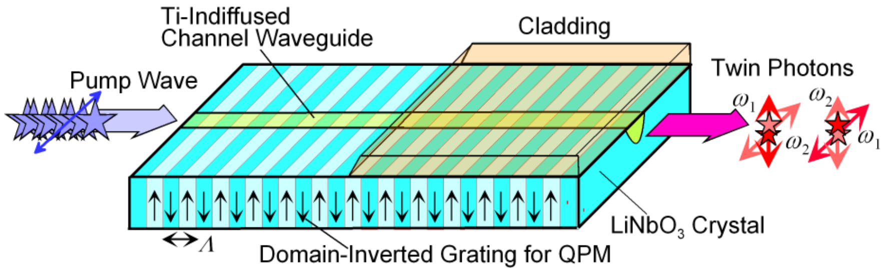

(b) Clad/Unclad type

Output state: $|\psi\rangle = \frac{1}{\sqrt{2}}\{|\underset{\lambda_{el}}{\mathrm{H}},\underset{\lambda_{es}}{\mathrm{V}}\rangle + \exp(i\Phi_0)|\underset{\lambda_{el}}{\mathrm{V}},\underset{\lambda_{es}}{\mathrm{H}}\rangle\}$

completely separated by DBS

Postselection-free two-λ polarization-entangled twin photons without spurious photon

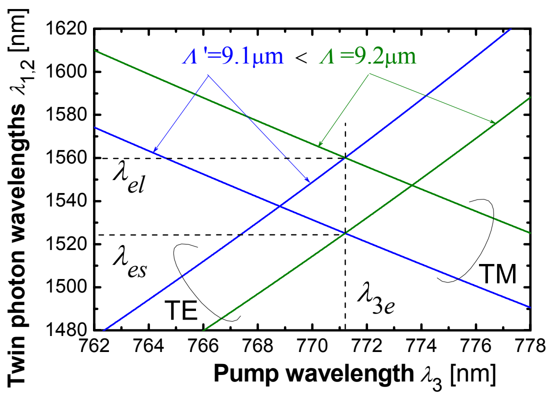

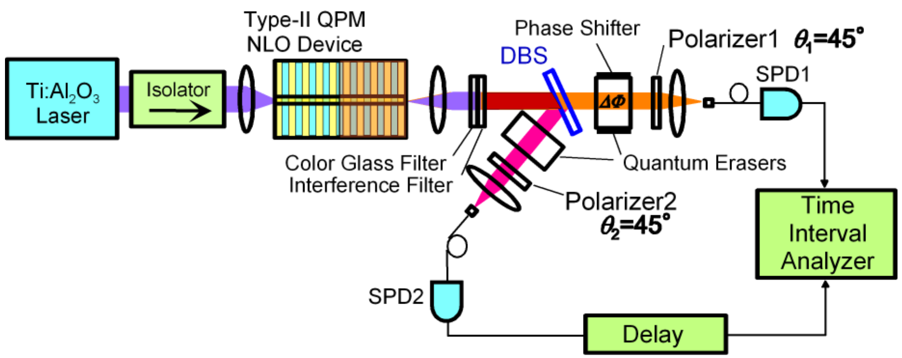

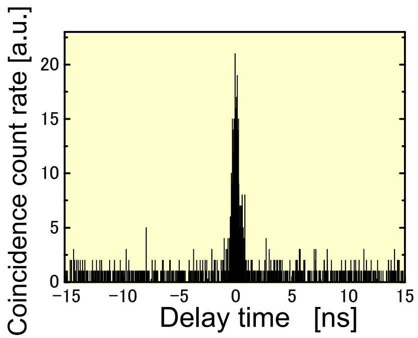

photon correlation

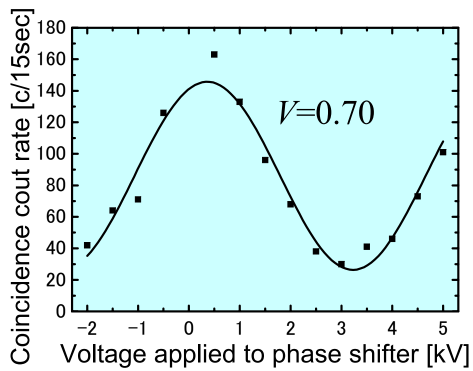

Quantum interference

T.Suhara et al. IEEE PTL **21**, 1096 2009.

Integrated Semiconductor Lasers

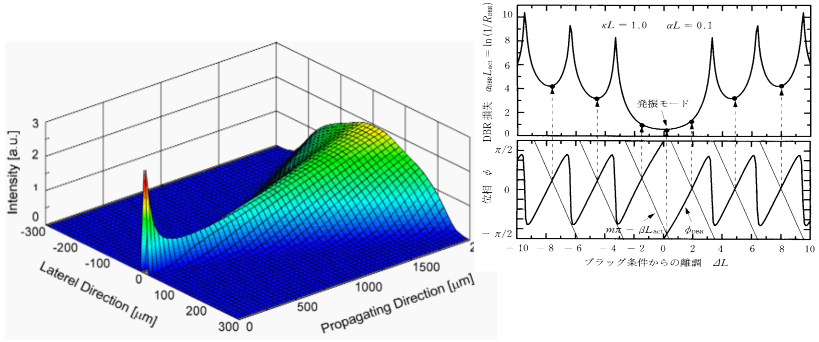

DFB/DBR Laser Simulation

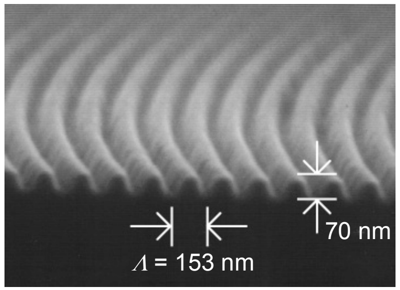

EB Fabrication of Nano Gratings

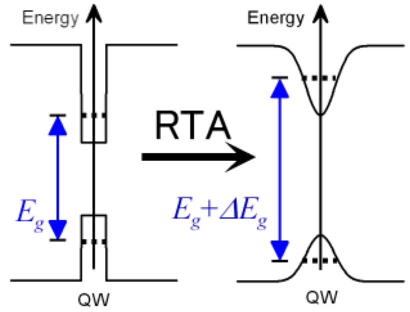

Selective Disordering of Quantum Well

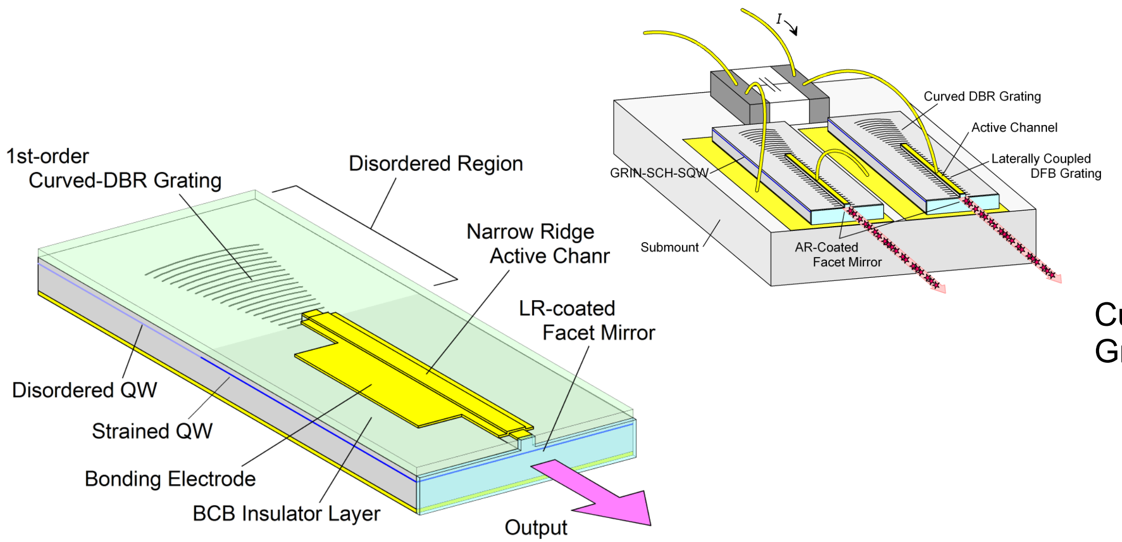

Integrated Semiconductor Lasers for Photonic Network and Quantum-Information

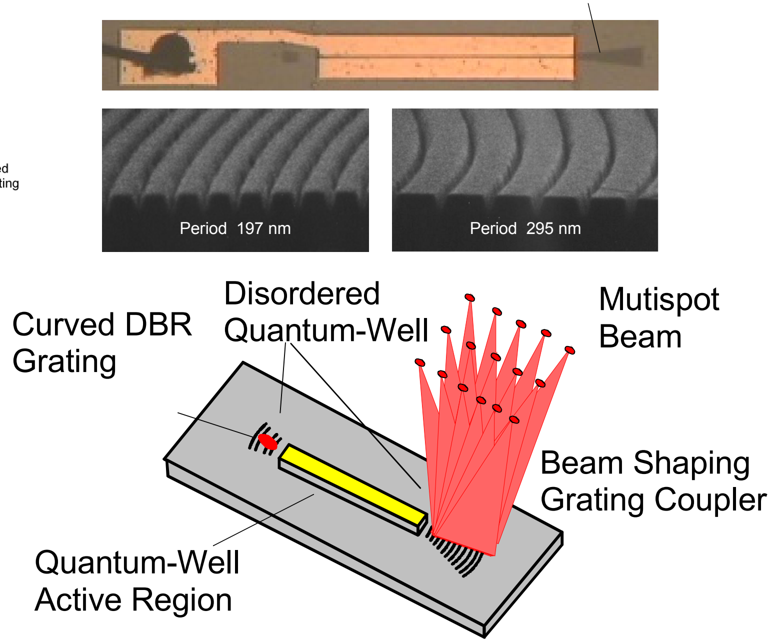

Integrated Semiconductor Lasers for Bio-Sensing

Monolithic Integrated-Optic Sensor Devices

Implementation of IO Sensor Devices by Integration of DFB/DBR Laser, Wavefront Conversion Elements and Photodetectors

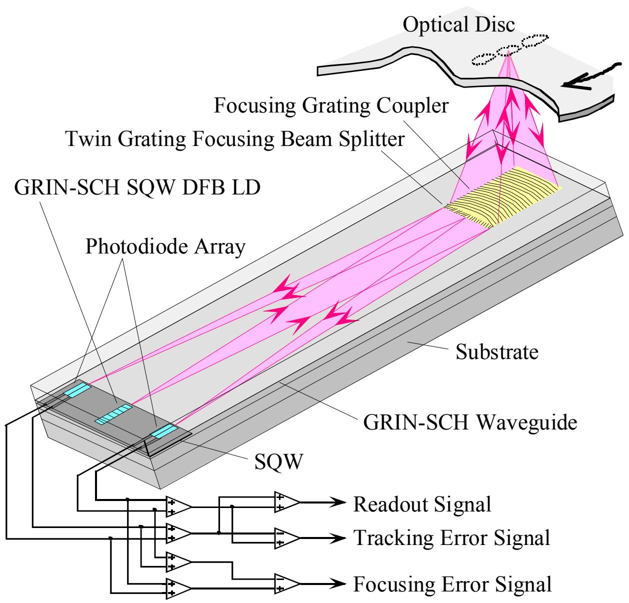

Monolithic Integrated-Optic Disc Pickup Head

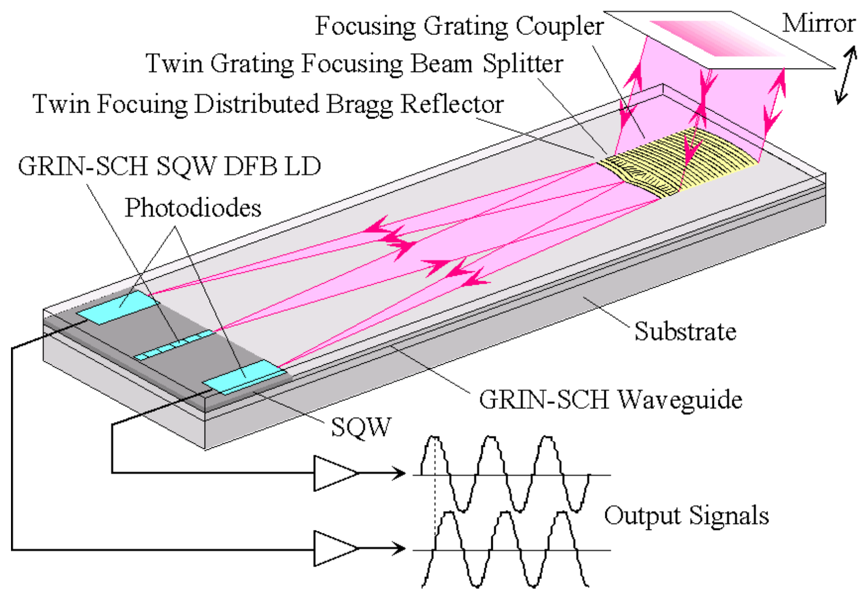

Monolithic Integrated-Optic Interferometer Posision/Displacement Sensor

Design Fabrication and Improvement of Novel Semiconductor Lasers

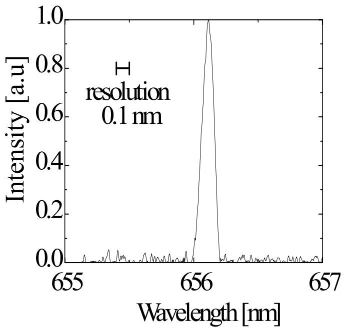

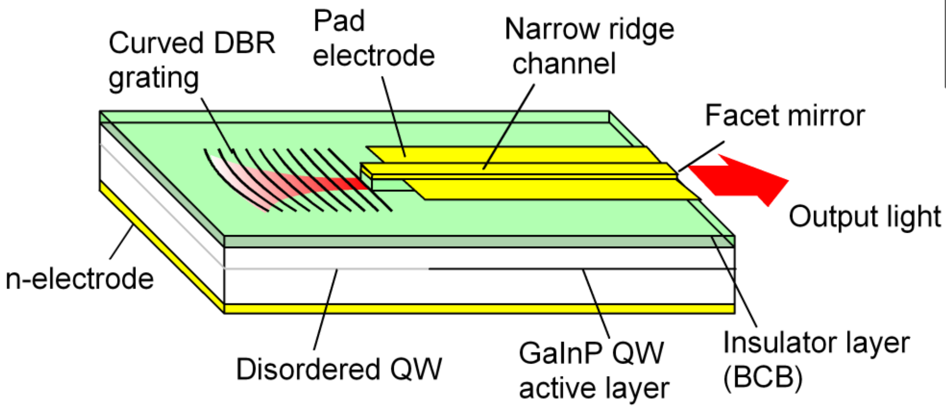

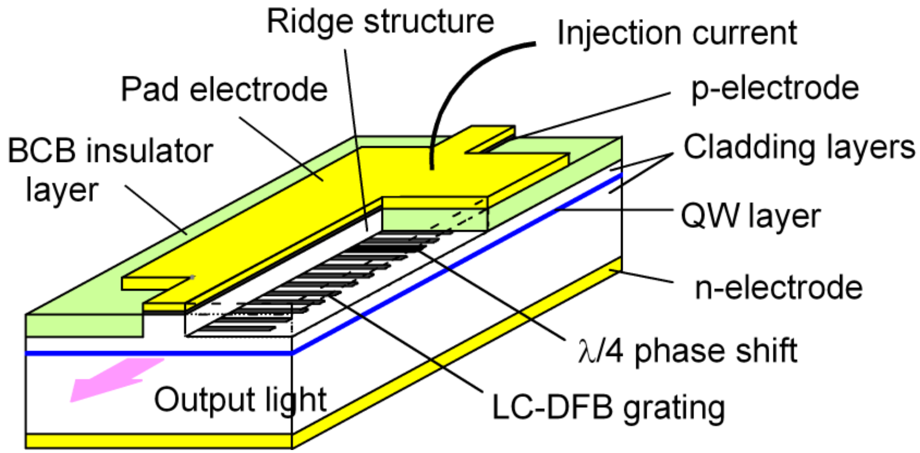

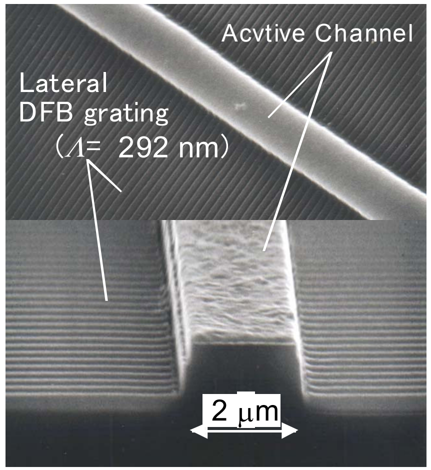

Red light emission DBR Laser

44mW output

for integrated optical memory

integrated biosensing devices

Lateral Coupling DFB Laser

19mW output , 46dB SMSR

Integrated High-Power High Coherence Semiconductor Lasers

Master Oscillator Power Amplifier with integrated Outcoupler

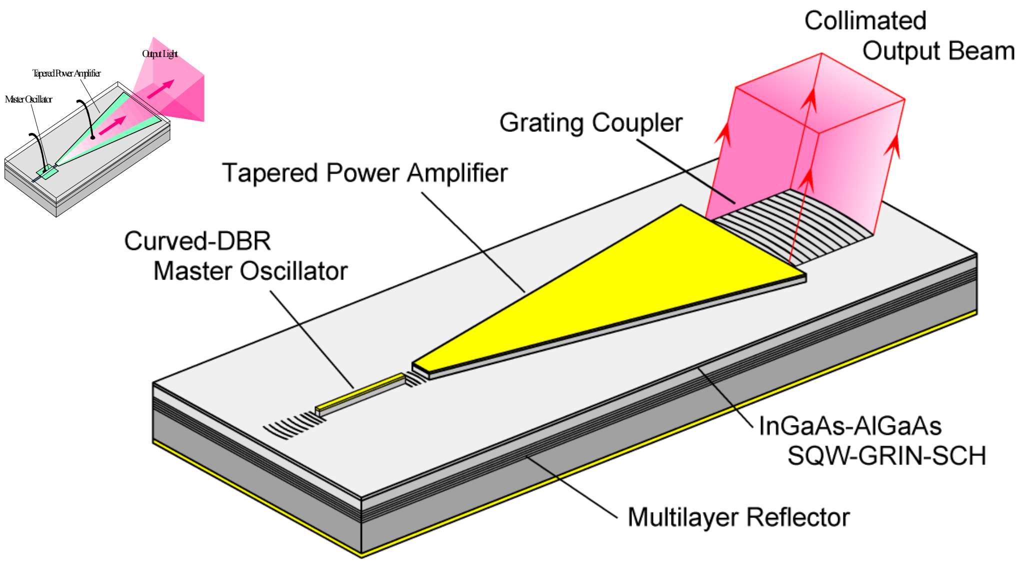

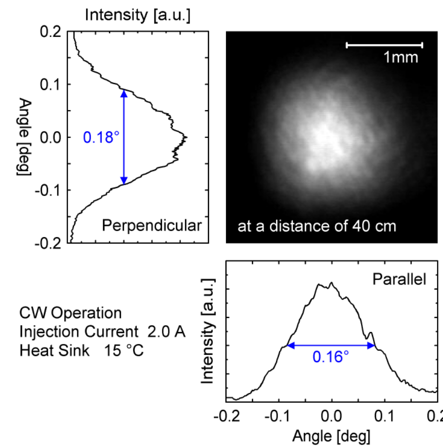

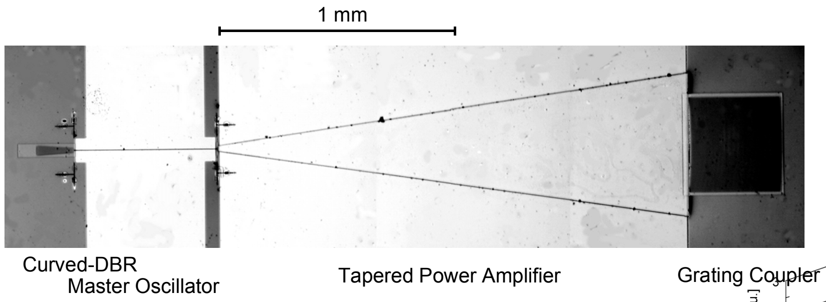

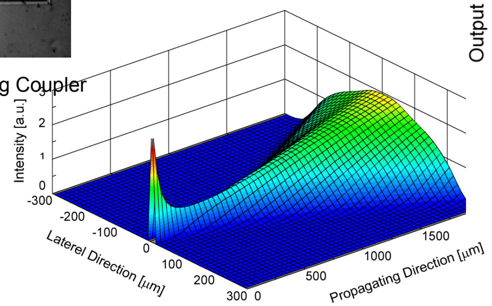

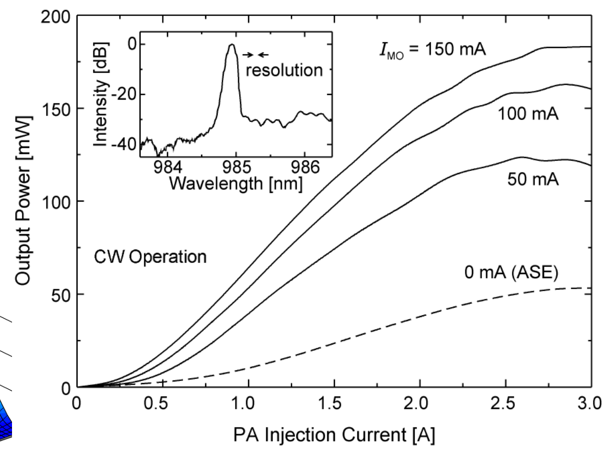

Integrated High-Power High Coherence Semiconductor Lasers

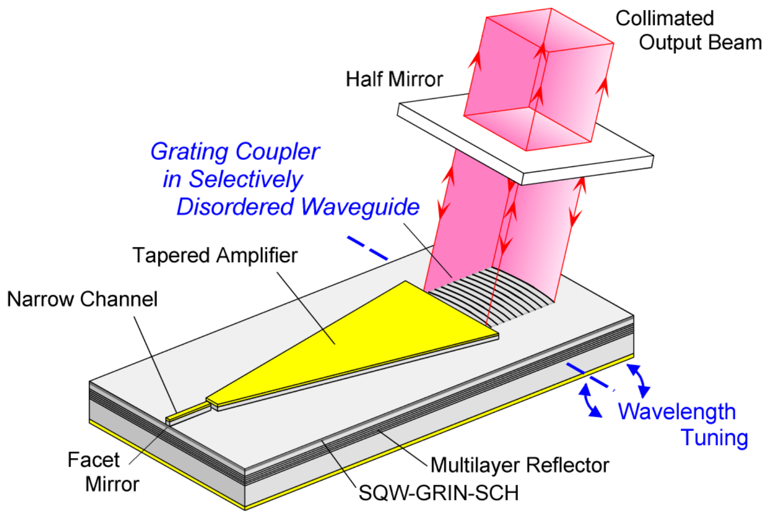

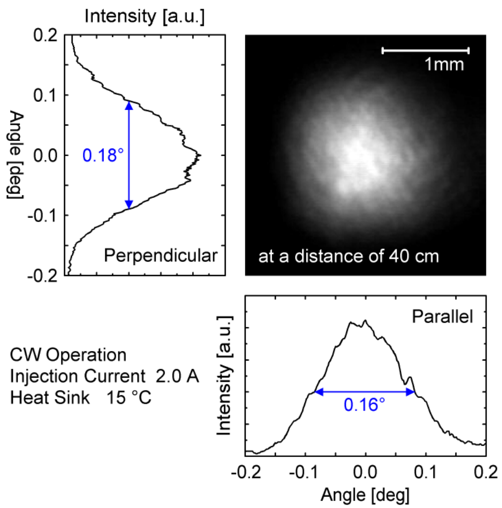

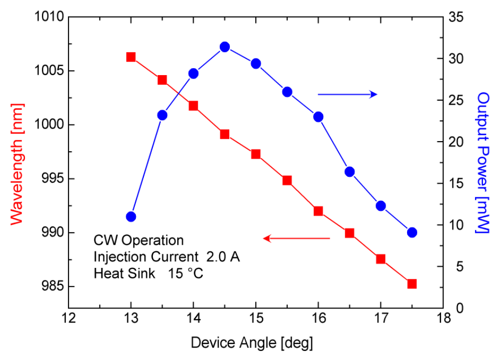

Extended Cavity Tunable Laser

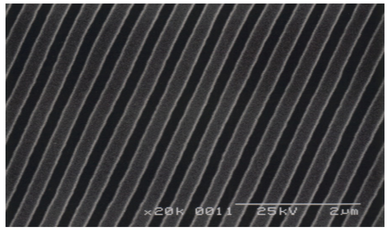

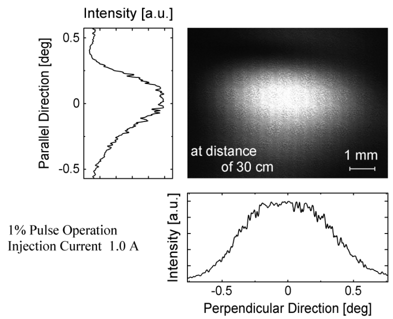

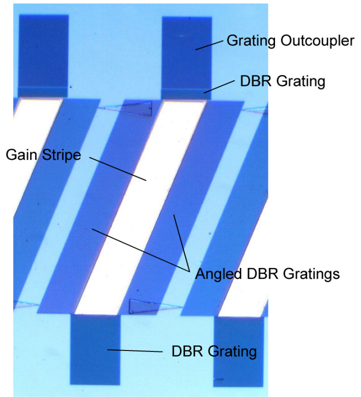

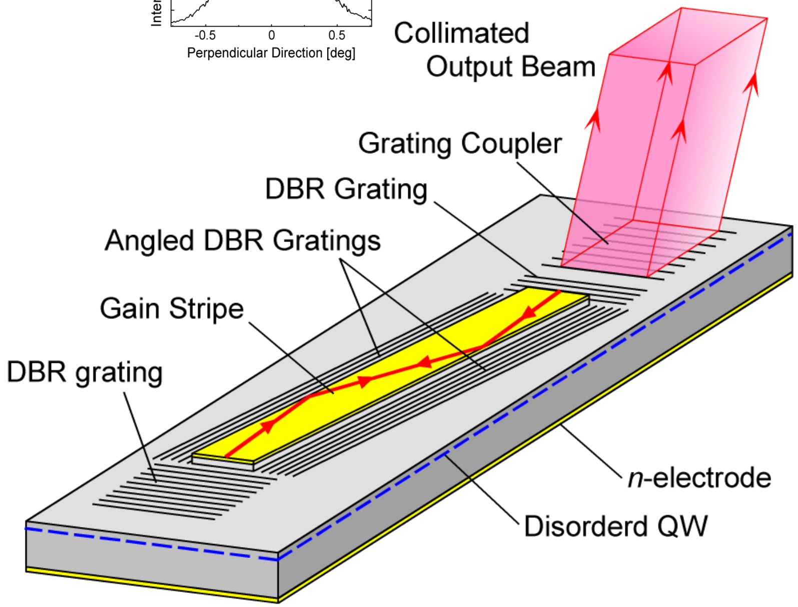

Broad-Area DBR Laser

InGaAs QW DBR Laser for Squeezed Light Generation

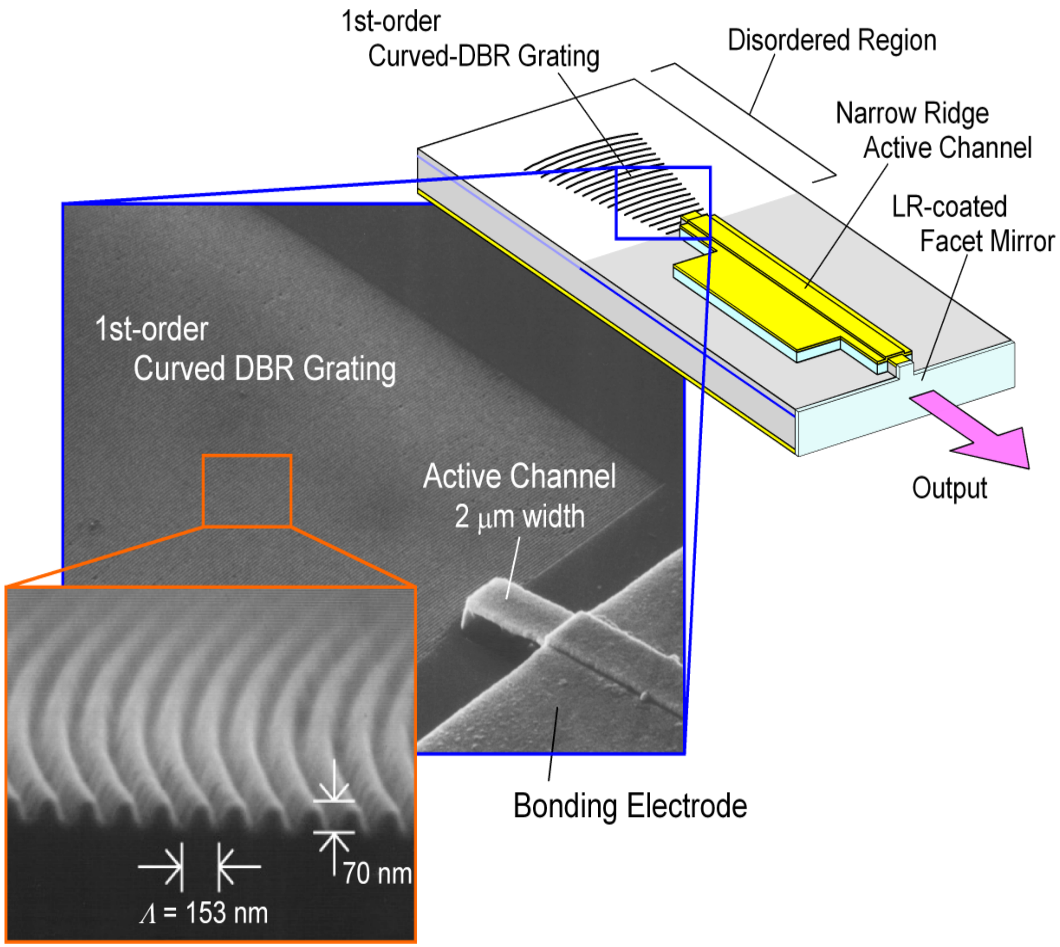

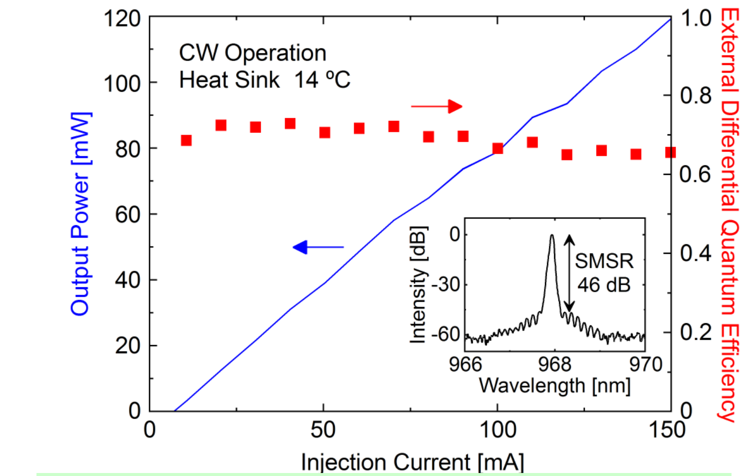

I_{th}=7mA η_d~0.63 Max I/I_{th}=21

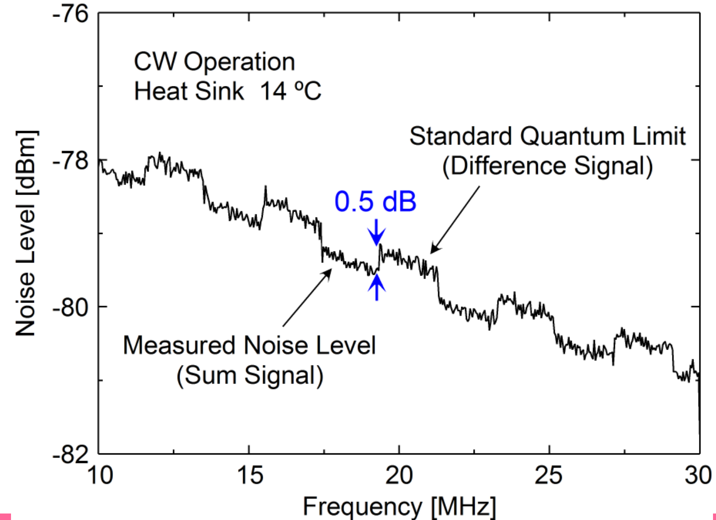

Generation of Squeezed Light

External Quantum Efficiency 74%
Side Mode Suppression 52 dB
Maximum Output Power 250 mW
Accomplished

M.Uemukai, et al. IEEE JSTQE, 11, 1143, 2005

Surface-Emitting Red DBR Laser and Application to Biomolecular Sensing

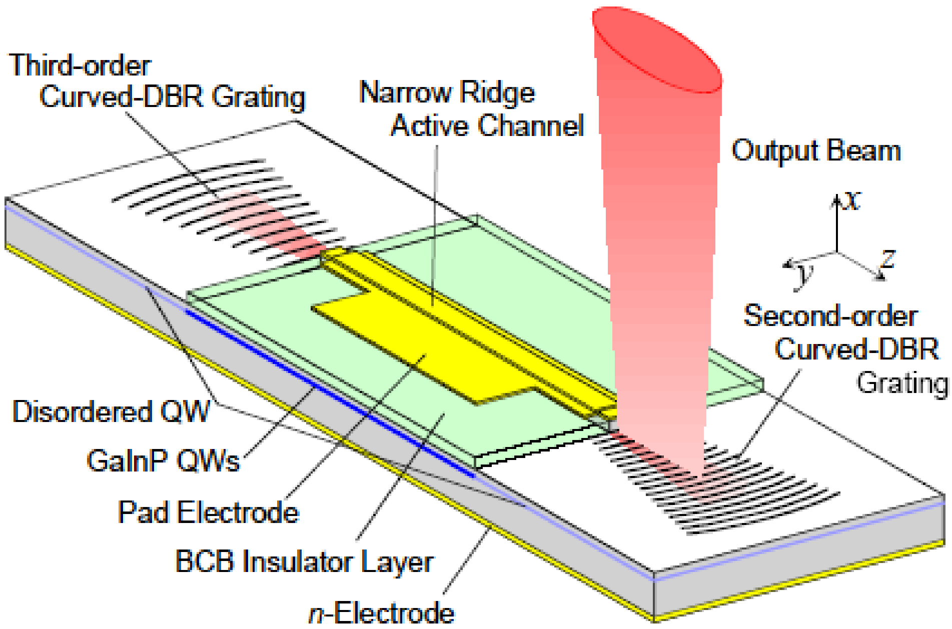

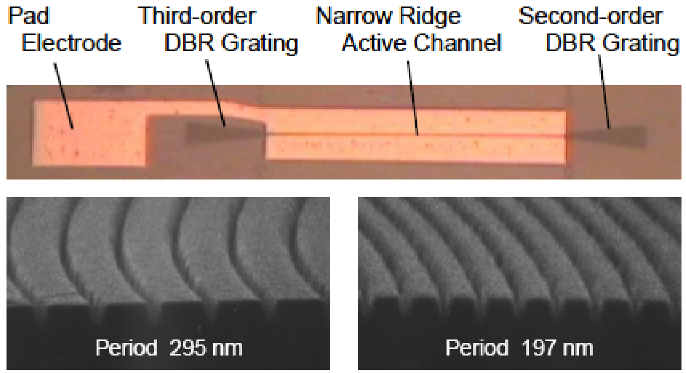

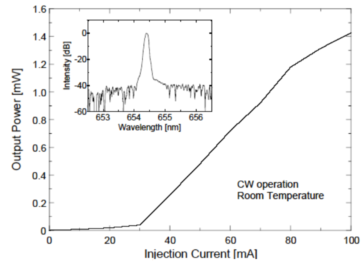

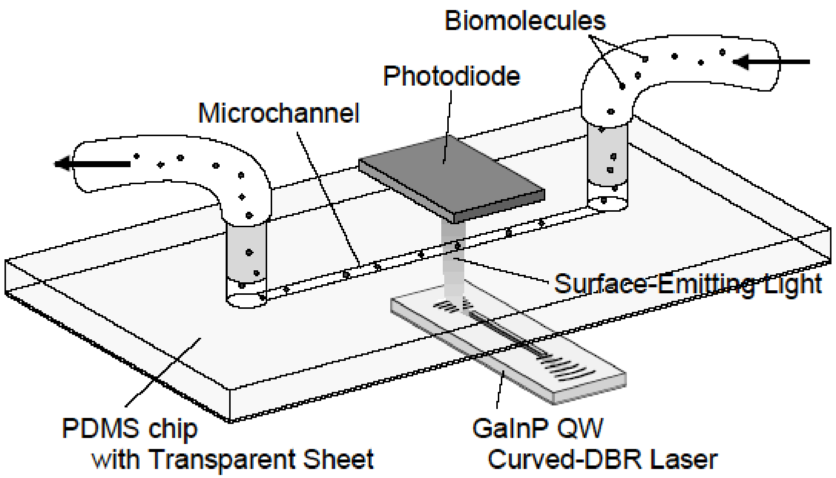

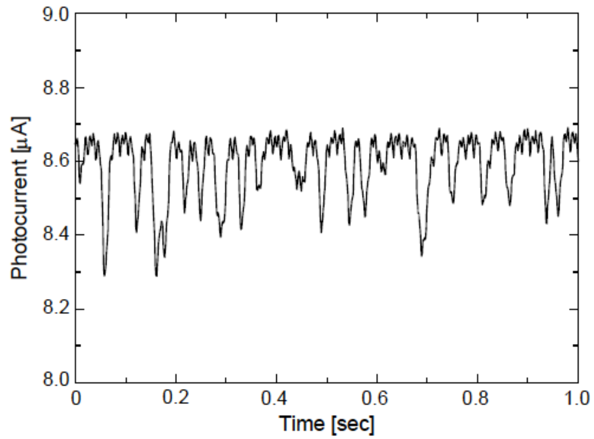

M.Uemukai et al. JJAP **45**, 6738, 2009

DBR laser with multispot focusing grating coupler

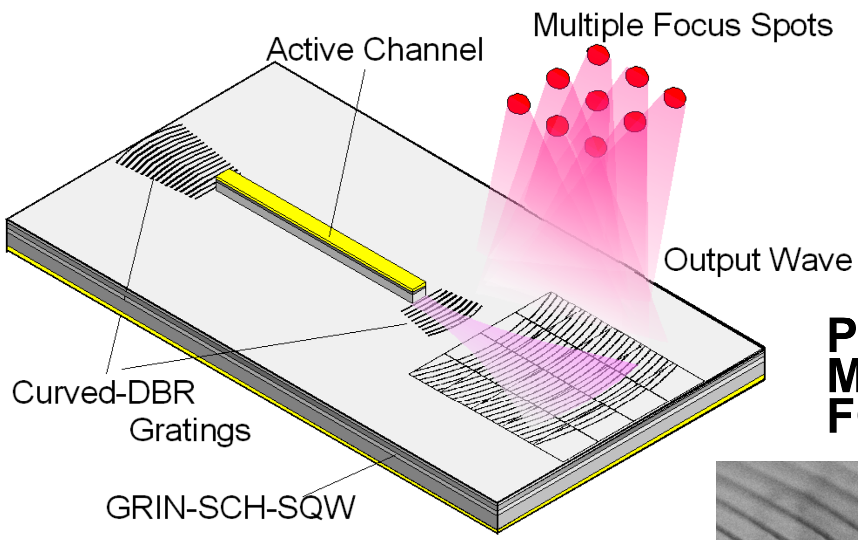

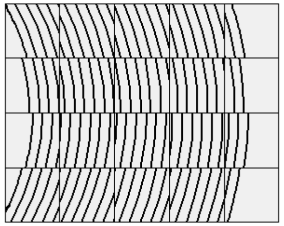

Phase-shifted Multispot FGC

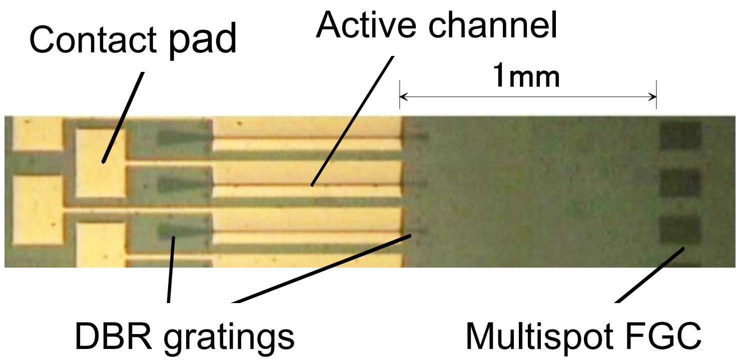

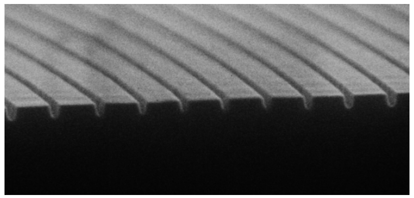

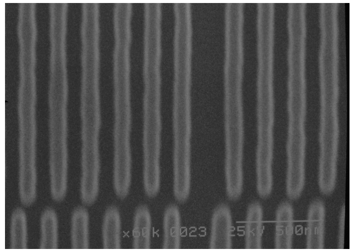

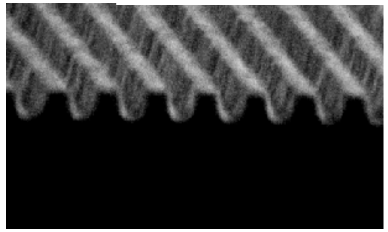

Λ～191nm

d～100nm

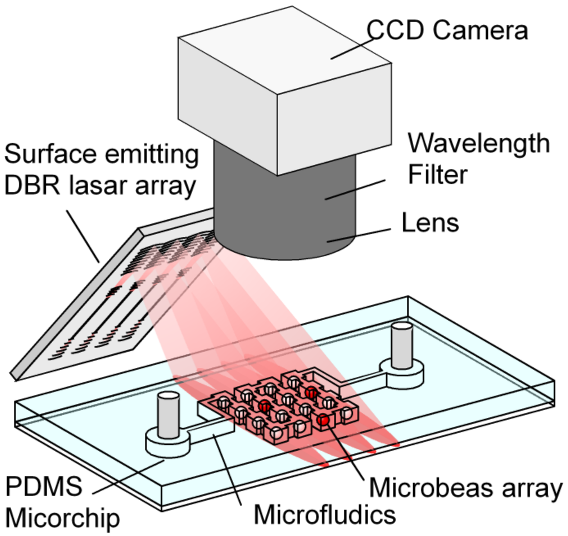

Application to biosensing

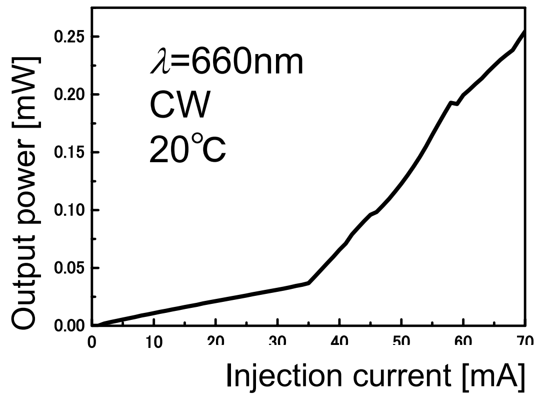

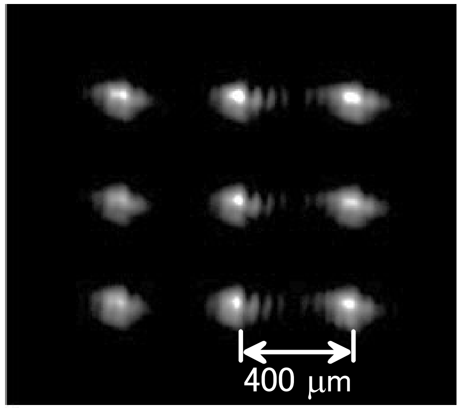

S.Takushima et al. JJAP **48**, 030206, 2009

Integrated twin DBR laser for THz wave generation